



## OPEN

SUBJECT AREAS:  
GENE EXPRESSION  
CHEMICAL ENGINEERINGReceived  
18 July 2014Accepted  
3 November 2014Published  
24 November 2014Correspondence and  
requests for materials  
should be addressed to  
S.L.C. (chensl@ysfri.  
ac.cn)

# Cloning and characterization of *wnt4a* gene and evidence for positive selection in half-smooth tongue sole (*Cynoglossus semilaevis*)

Qiaomu Hu<sup>1,2</sup>, Ying Zhu<sup>1</sup>, Yang Liu<sup>1</sup>, Na Wang<sup>1</sup> & Songlin Chen<sup>1</sup><sup>1</sup>Yellow Sea Fisheries Research Institute, Chinese Academy of Fishery Sciences; Key Laboratory of Sustainable Development of Marine Fisheries, Ministry of Agriculture, Qingdao 266071, China, <sup>2</sup>Yangtze River Fisheries Research Institute, Chinese Academy of Fishery Sciences, Wuhan 430223, China.

*Wnt4* gene plays a role in developmental processes in mammals. However, little is known regarding its function in teleosts. We cloned and characterized the full-length half-smooth tongue sole (*Cynoglossus semilaevis*) *wnt4a* gene (*CS-wnt4a*). *CS-wnt4a* cDNA was 1746 bp in length encoding 353aa. *CS-wnt4a* expression level was highest in the testis, and gradually increased in the developing gonads until 1 year of age. *In situ* hybridization revealed that *CS-wnt4a* expression level was highest in stage II oocytes and sperm in the adult ovary and testis, respectively. *CS-wnt4a* expression level was significantly up-regulated in the gonads after exposure to high temperature. The level of methylation of the *CS-wnt4a* first exon was negatively correlated with the expression of *CS-wnt4a*. The branch-site model suggested that vertebrate *wnt4a* differed significantly from that of *wnt4b*, and that the selective pressures differed between ancestral aquatic and terrestrial organisms. Two positively selected sites were found in the ancestral lineages of teleost fish, but none in the ancestral lineages of mammals. One positively selected site was located on the  $\alpha$ -helices of the 3D structure, the other on the random coil. Our results are of value for further study of the function of *wnt4* and the mechanism of selection.

**W**nt4 (wingless-type MMTV integration site family, member 4) plays a crucial role in ovarian differentiation in mammals. In mice, *wnt4* is expressed in the mesonephros, the gonad, and the Müllerian duct, suggesting that *wnt4* plays an important role in development of the reproductive system<sup>1</sup>. The absence of *wnt4* in female embryos (XX) leads to masculinization<sup>2</sup>. However, over-expression of *wnt4* does not result in sex reversal in males<sup>3</sup>. The phenotype of human female that have a *wnt4* mutation is similar to that of female *wnt4* knockout mice<sup>4</sup>. Individuals who have a duplication of the chromosome containing the *wnt4* gene exhibit sex reversal<sup>5,6</sup>. In addition to humans and mice, ovarian *wnt4* expression has been reported in a range of mammals, including the bonnet macaque (*Macaca radiata*)<sup>7</sup>, tammar wallaby (*Macropus eugenii*)<sup>8</sup>, and goats (*Capraeagrus hircus*)<sup>9</sup>. These studies have focused primarily on the role of *wnt4* in ovarian differentiation. In contrast, little is known about the potential role in testis development. In mice, Sertoli cell differentiation is compromised in *wnt4* mutant testes. In this instance, the expression of the testis-determining gene *Sry* was down-regulation, whereas expression of the Sertoli cell marker genes, *Sox9* and *Dhh*, was up-regulated<sup>10</sup>. These observations suggest that *wnt4* is involved in mammalian testis determination. In mice that have transgenic mis-expression of *wnt4*, Leydig cell differentiation is not affected but migration of the steroidogenic adrenal precursors into the gonad is repressed<sup>3</sup>. Similarly, transgenic mice that have a human *wnt4* gene exhibit a dramatic reduction in steroidogenic acute regulatory protein expression and testicular androgen levels<sup>11</sup>. These observations suggest that *wnt4* acts as an anti-male factor<sup>12</sup>. Taken together, the studies described above provide evidence that *wnt4* plays an important role in gonad development. *Wnt4* function has also been evaluated in other organisms, including the millipedes *Glomeris marginata* (*Myriapoda: Diplopoda*)<sup>13</sup>, frogs (*Rana rugosa*)<sup>14</sup>, garden lizard (*Calotes versicolor*)<sup>15</sup> and chickens (*Gallus gallus*)<sup>16</sup>. In teleosts, the role of *wnt4* in gonad development has only been studied in rainbow trout (*Oncorhynchus mykiss*)<sup>17</sup>, and the protandrous black porgy (*Acanthopagrus schlegelii*)<sup>18</sup>. Interestingly, in most teleosts, the *wnt4* gene was duplicated due to the teleost-specific whole-genome duplication<sup>17</sup>. This second duplication resulted in two paralogs, *wnt4a* and *wnt4b*. Additionally, a third *wnt4* gene,



*wnt4a2*, has been documented in some teleost species<sup>17</sup>. The two *wnt4a* genes (*wnt4a1* and *wnt4a2*) exhibit dimorphic expression in the gonad. This can be explained in two ways. Gene duplication may have led to new function for the gene (neo-functionalization) which may be different from the paralogs's function<sup>19–21</sup>. Alternatively, genome duplication can lead to a high rate of molecular evolution in fish, after which the duplicated gene causes functional division of the tasks<sup>22</sup>.

Half-smooth tongue sole (*Cynoglossus semilaevis*) is an economically important farmed marine fish that are widely distributed along the Chinese coast. Because of their desirable taste and nutritional and economic value, it was selected for aquaculture. Half-smooth tongue sole exhibit significant sexual dimorphism in growth whereby the female grows faster than the male<sup>23</sup>. Thus, breeding all female or a high proportion female stock has been proposed as a way to increase production. To achieve this, there is a need to better understand the mechanism of sex determination and sex differentiation. In the previous research, we demonstrated that exposure of genetic female half-smooth tongue sole to high temperature resulted in a phenotypic male with the female genotype (neomale: ZW)<sup>24</sup>. Interestingly, methylation appears to play an important role in sex determination and sex reversal<sup>25</sup>. Additionally, we have measured the expression of a number of sex related genes, including *Foxl2*, *Cyp19a1*, *Sox9*, *Ubc9*, and *Dmrt1* during gonadal development<sup>26–30</sup>. Furthermore, the whole genomic sequence of the half-smooth tongue sole was sequenced<sup>30</sup>. Comparison of the tongue sole sex chromosomes with those of mammals and birds during the early phase of sex chromosome evolution has revealed the loss of large numbers of genes in tongue sole during sex chromosome evolution<sup>30</sup>. Despite the availability of the whole genomic sequence, the mechanism of its sex determination remains unclear.

The role of the *wnt4* gene in half-smooth tongue sole, particularly in sex determination and gonad differentiation, remains uncharacterized. Our objective was to identify and characterize the role of the *CS-wnt4a* in sex determination and gonadal differentiation. We measured the pattern of tissue expression and the temporal pattern of expression in the gonads. Additionally, we evaluated the correlation between promoter methylation and *CS-wnt4a* expression. We found evidence for positive selection of *wnt4* genes in the various groups: teleosts, mammals and invertebrates.

## Results

**cDNA characterization of half-smooth tongue sole *CS-wnt4a*.** We obtained the full length *CS-wnt4a* gene following RACE primer amplification (Table S1). The complete cDNA sequence of *CS-wnt4a* was 1746 nucleotides in length (GenBank accession No: KJ825677), consisting of a 5'-untranslated region (UTR) of 435 bp and a 3'UTR of 252 bp. The open reading frame (ORF) was 1059 bp in length and encoded a protein of 353 amino acids with a predicted molecular weight of 39.38 kDa. The position of the signal peptide was predicted and the signal cleavage site was identified between Ala<sup>22</sup> and Ser<sup>23</sup> (Fig. S1). A typical WNT domain (containing 308 amino acids) was identified in *CS-wnt4a* gene. Additionally, twenty glycosylation sites (Thr-2, Asn-21, Ser-23, Asn-24, Ser-60, Asn-88, Thr-103, Ser-116, Ser-146, Ser-168, Ser-181, Ser-182, Asn-187, Asn-191, Ser-200, Thr-219, Asn-232, Thr-252, Thr-286, Asn-298, and Thr-350) were predicted using bio-informatics (Fig. S1).

**Tissue distribution and temporal expression in the gonads.** We measured mRNA levels in 13 tissues and throughout development in the gonads of the half-smooth tongue sole. The level of expression differed significantly among the tissues ( $p < 0.05$ ). The level of expression was high in the testis (T), moderate in the gill (G), skin (S), brain (B), pituitary (P), and ovary (O), and low in the remaining tissues (Fig. 1A).

To measure the expression of *CS-wnt4a* genes during the period of gonad differentiation, *CS-wnt4a* expression was detected in female and male gonads at different stages by qRT-PCR. The level of expression was weak from 7 d (7D) to 48 d (48D) after hatch, then increased rapidly at 70D and continued to increase gradually up to 1 year (1Y). The level of expression was highest at 1Y, after which there was a rapid decrease at 2 years (2Y) (Fig. 1B). There was no difference in *CS-wnt4a* expression between female gonads and male gonads from 7D to 160D. However, expression was significantly higher in male gonads than in female gonads from 1–2Y ( $p < 0.05$ ).

The location of *CS-wnt4a* expression in the gonad was determined using *in situ* hybridization (ISH) in adult tongue sole. The adult tongue sole ovary contains somatic cell and several different developmental stages of oocytes from small (stage I) to mature oocytes (stage IV). ISH revealed that *CS-wnt4a* expression was strong in stage I–III oocytes, but weak in stage IV oocytes (Fig. 1C). The strongest signal was observed at stage II (Fig. 1D). The distribution of *CS-wnt4a* RNA expression was uniform in stages I–III oocytes, and perinuclear in stage IV oocytes (Fig. 1D). The adult tongue sole testis contain spermatogonia (sg), primary spermatocytes (psc), secondary spermatocytes (ssc), spermatids (st), and sperm (sm). The transcription of *CS-wnt4a* was detected in sg, psc, ssc, st, and sm. The signal was strong in sm, moderate in ssc and st, and weak in sg and psc (Fig. 1E and F). We did not detect any signal from the sense probe (Fig. S2).

**Expression and methylation during sex reversal.** We measured *CS-wnt4a* expression in the testis and ovary of normal males and females and the testis of neomales. *CS-wnt4a* expression was high in the testis of neomales, moderate in the testis of normal males, and low in the ovary of normal females (Fig. 2A).

To test the relationship between methylation and expression, the first exon of *CS-wnt4a* was examined and the 298 bp CpG dinucleotide was selected (Fig. S1). The level of gonad methylation in the *CS-wnt4a* first exon was determined using bisulfite sequencing in one-year-old half-smooth tongue sole males, females, and neomales. There was a significant difference in average DNA methylation levels in the half-smooth tongue sole *CS-wnt4a* first exon among these three groups. The level of *CS-wnt4a* methylation was twice as high in females as in sex reversed tongue sole (mean  $\pm$  SEM: 47.29  $\pm$  0.043% versus 19.11  $\pm$  0.099%, Fig. S3). In addition, the levels were significantly higher in females than in males (27.02  $\pm$  0.079%) (Fig. 2B). Interestingly, the level of RNA transcription was negatively correlated with the level of methylation suggesting that methylation of the *CS-wnt4a* first exon inhibits RNA transcription.

**Multiple alignment and phylogenetic analysis.** After a comprehensive search in GenBank and Ensemble, we downloaded 36 sequences of *wnt4* in 28 species, including *Takifugu rubripes*, *Gasterosteus aculeatus*, *Oreochromis niloticus*, *Tetraodon nigrovirdis*, *Haplochromis burtoni*, *Maylandia zebra*, *Dicentrarchus labrax*, *Oncorhynchus mykiss*, *Xiphophorus maculatus*, *Oryzias latipes*, *Gadus morhua*, *Danio rerio*, *Rattus norvegicus*, *Homo sapiens*, and *Macaca mulatta* (Table S2). The protein sequences were aligned (Fig. S4) in Clustalx to produce the phylogenetic tree of the *wnt4* genes using the Bayesian method. To evaluate clade support, we used the Bayesian posterior probability (PP) method. The sequences clustered in two main groups: a *wnt4a* cluster containing teleosts (pp = 0.90) and mammals (pp = 1.00), and a *wnt4b* cluster that contained only teleosts (Fig. 3).

**Molecular evolution analysis.** To analyze whether there were positively selected sites in the ancestral lineages of the *wnt4* gene tree, all vertebrate *wnt4* sequences were utilized to test whether different environments had affected the selective pressure on *wnt4* genes in ancestral lineages of aquatic or terrestrial organisms. Firstly, the  $\omega$  for all branches was 0.036 ( $p = 0$ , Table 1), suggesting that all

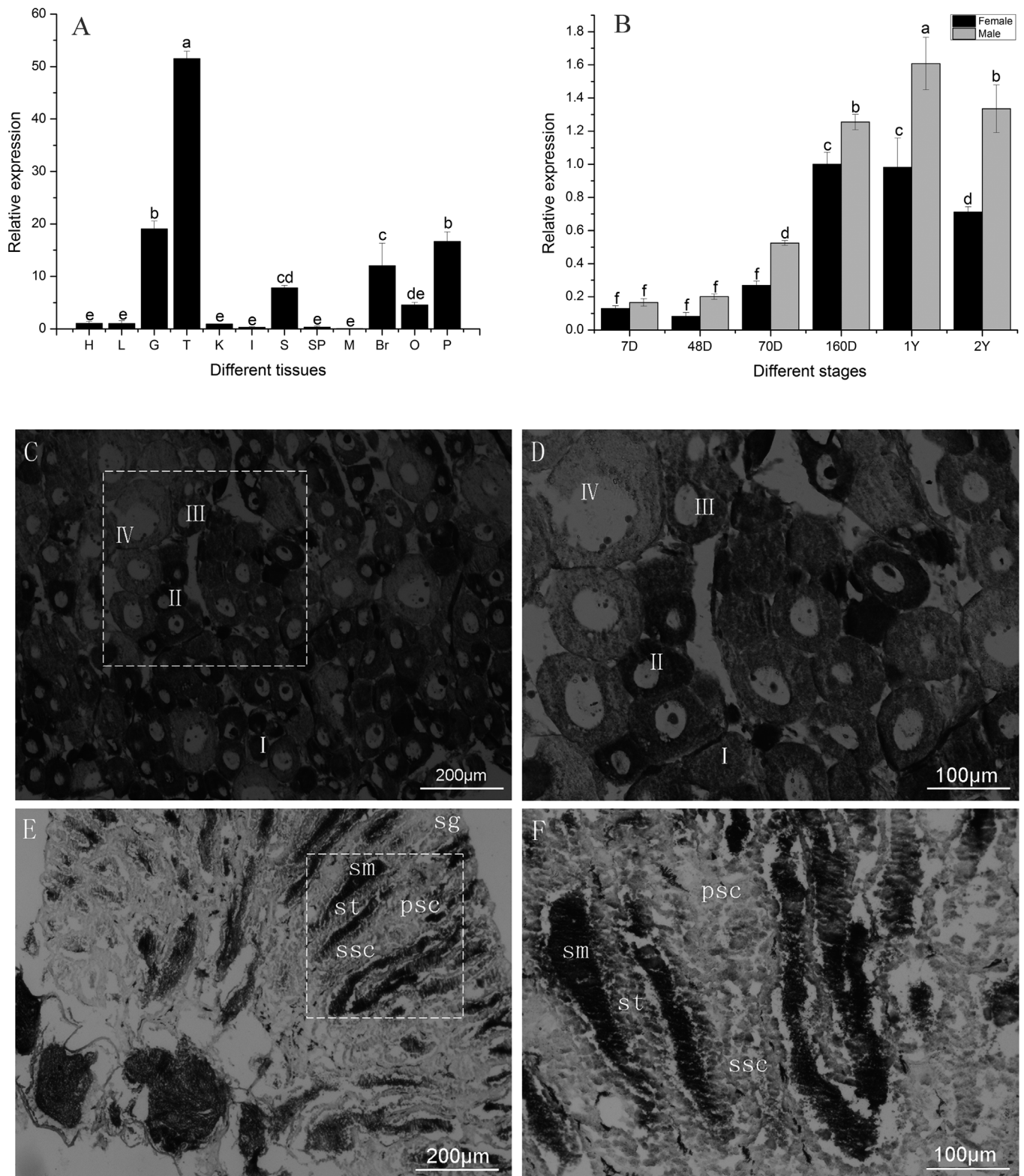


**Figure 1 | The expression of *CS-wnt4a* in *C.semilaervis*.** (A). The expression of *CS-wnt4a* in different tissues H: heart, L: liver, G: gill, S: skin, K: kidney, I: intestine, Br: brain, Sp: spleen, M: muscle, P: pituitary, O: ovary, T: testis. (B). The expression profile of *CS-wnt4a* at different developmental stages in the gonads was revealed by real-time quantitative PCR. 7D: 7 day age, 48D: 48 day age, 70D: 70 day age, 160D: 160 day age, 1Y: 1 year age, 2Y: 2 year age. (C) Low magnification showing the adult ovary architecture including four stages of oocytes by *in situ* hybridization: stage I–IV. (D) Large magnification of frame area in (C). (E) Low magnification showing the adult testis architecture including spermatogonia (sg), primary spermatocytes (psc), secondary spermatocytes (ssc), spermatids (st), and sperm (sm) by *in situ* hybridization. (F) Large magnification of frame area in (E) highlighting the distribution of *CS-wnt4a* RNA.

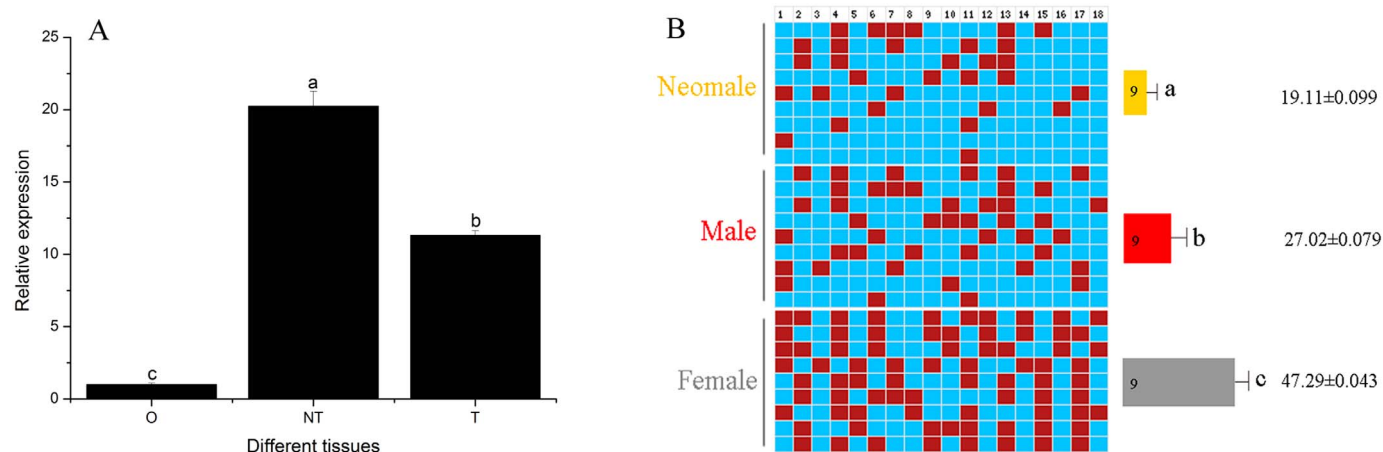


**Figure 2** | (A). Expression analysis of *CS-wnt4a* by relative quantitative real-time PCR in gonads of females, males, and neomales in 1-year-old individuals. O: ovary, T: testis, NT: neomale testis. Bars with different letters are significantly different ( $p < 0.05$ ). (B). Differences in *CS-wnt4a* first exon methylation in the gonads of females, males, and neomales at 1 year of age. Numbers in the first row indicate CpG positions. The red box and blue box denote methylated and unmethylated positions, respectively. The number inside the bar indicates sample size. Results represent the mean  $\pm$  SE. Groups with different letters are significantly different ( $P < 0.05$ ).

*wnt4* genes were under purifying selection. Secondly, comparison of the free-ratio model with the one ratio model revealed that each branch has independent  $\omega$  values ( $p = 5.93715E-07$ ). Lastly, the branch-site model was applied to determine whether a positive selection site was existed in the lineages of vertebrate, *wnt4a*, *wnt4b*, mammalian and teleost. We found evidence for positive selection in *wnt4a*, *wnt4b* and teleosts (Table 1). A site model was then used to identify the positive selection site in the *wnt4* gene of mammals and teleosts. In mammals, the likelihood ratio test (LRT) value was obtained from comparison of the two models. The M3-M0 comparison was 107.74 ( $p < 0.01$  Table 2). The M2a-M1a and M7-M8 comparison was 0 ( $p = 1$ ), and M8 and M2a were rejected. A positive selection site was not found in mammals. In teleosts, 4 and 2 positively selected sites were found in M3-M0 and M8-M7, respectively, with LRT values of 212.94 ( $p < 0.01$ ) and 20.48 ( $p < 0.01$ ). Conversely, no positively selected site was found in the M2a-M1a comparison and the LRT value was 0 ( $p = 1$ ) (Table 2).

**Structure analysis and positive selection sites on the three dimensional structure.** To map positively selected sites onto *CS-wnt4a* 3D model and present the results of our study more visualized, two positively selected sites were identified and mapped onto the surface of the 3D structure (Fig. 4). The 3D structure contained 8  $\alpha$ -helices and 4 $\beta$ -strands, and one positively selected site (94T) on the  $\alpha$ -helices, the other one (39D) on the random coil.

## Discussion

*Wnt4* genes are involved in many important developmental processes in vertebrates, including reproduction, sex determination, and sex inversion<sup>13,31,32</sup>. New functions for *wnt4* genes have been found in mammals, fishes, and other vertebrates<sup>33–35</sup>. *Wnt4* genes have been described in some teleosts, though few species have been comprehensively and systematically studied. We cloned *CS-wnt4a*, and then evaluated the pattern of expression and methylation. The open reading frame shared many characteristic features with *wnt4a* from other vertebrates. The putative conservative domain of *CS-wnt4a* possessed high identity with *wnt4a* from other species (Fig. S4). *CS-wnt4a* was divided into two regions, a signal peptide and a mature peptide. Additionally, twenty glycosylation sites were found in the *CS-wnt4a* putative amino acid peptide. The number of glycosylation sites is positively associated with the diversity of protein function<sup>36,37</sup>, suggesting that the *wnt4a* gene has a variety of biological functions.

*Wnt4* gene is found in both invertebrates<sup>14,38,39</sup> and vertebrates<sup>11,40,41</sup>. Our results demonstrated that most teleost fish have two *wnt4* genes, *wnt4a* and *wnt4b*, whereas invertebrates and other vertebrates possess only a single *wnt4* gene. This suggested that teleost fish underwent a whole-genome duplication that yielded two *wnt4* paralogs<sup>42</sup>. The relationship of a duplicated *wnt4* gene (*wnt4b*), which formed a cluster on one branch with mammals (Fig. 4), was not supported by the phylogenetic analysis. This inconsistent phenomenon could be explained by a long-branch attraction effect due to the divergence of *wnt4b* sequences<sup>43</sup>. A high rate of molecular evolution has occurred during genome duplication in fish such that duplicate genes are often associated with a functional shift<sup>24</sup>. An additional duplication of *wnt4* occurred in some teleost species resulting in two copies of the *wnt4a* gene, *wnt4a1* and *wnt4a2*<sup>17</sup>.

In half-smooth tongue sole, *wnt4a* was primarily expressed in the gonads, gill, and brain. This is consistent with observations in other teleost fish, including zebrafish<sup>44</sup> and rainbow trout<sup>17</sup>. Similarly, *wnt4* is expressed at a high level in the testis and moderate level in the ovary of the tamar wallaby<sup>45</sup>. The level of *CS-wnt4a* expression increased significantly at day 70 then increased gradually up to 1 year. The pattern of expression was consistent with the developmental process in the gonads. For example, proliferation is most rapid in the ovary at 62 days and spermatogonial cells begin mitosis at 80 days. Additionally, the level of *CS-wnt4a* expression was significantly higher in the testis than in the ovary at both 1 and 2 years of age ( $p < 0.05$ ). In mice, steroidogenesis occurs earlier in male embryonic gonads than in female embryonic gonads. Steroidogenic cell recruitment and steroidogenic gene expression appears to be inhibited by elevated expression of *wnt4a* in the future ovary<sup>3,46</sup>. However, in half-smooth tongue sole, steroidogenesis begins earlier in female embryonic gonads than in male embryonic gonads<sup>47</sup>. So, we speculated that the over-expression of *CS-wnt4a* in male half-smooth tongue sole gonads might cause a delay of steroidogenesis in males. A similar phenomenon was reported in rainbow trout<sup>11</sup>. Therefore, we speculated that *CS-wnt4a* expression was associated with the gonad differentiation in the half-smooth tongue sole. Indeed, the role of *wnt4* in gonad differentiation has been demonstrated in the frog (*Rana rugosa*)<sup>16</sup>, black porgy (*Acanthopagrus schlegelii*)<sup>18</sup>, and rainbow trout (*Oncorhynchus mykiss*)<sup>17</sup>.

*In situ* hybridization of the adult ovary revealed that *CS-wnt4a* was primarily expressed in the oocytes. The strongest signal was observed in stage II oocytes. *CS-wnt4a* expression increased gradually from stage I and then decreased after expression peaked during stage II

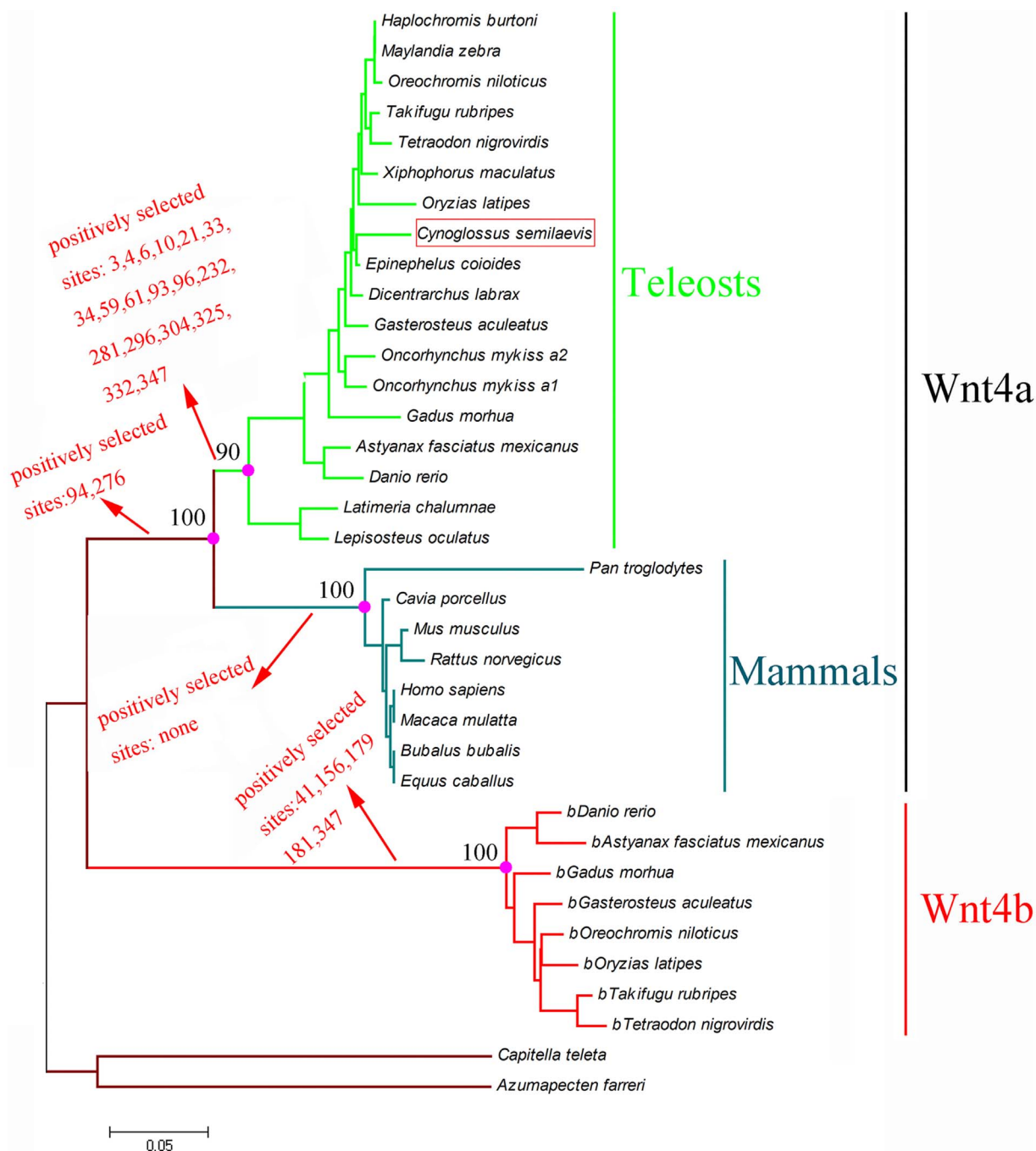


**Figure 3** | Phylogenetic tree of the nucleotide sequence of *wnt4* reconstructed by the Bayesian approach.

(Fig. 1). In the testis, *CS-wnt4a* expression was identified during all stages of spermatogenesis. The signal strength gradually increased during spermatogenesis and peaked in the mature sperm. These observations were consistent with the pattern of *CS-wnt4a* expression determined by qRT-PCR.

To evaluate whether *CS-wnt4a* played a role in sex reversal, we measured the level of *CS-wnt4a* transcripts in the gonads of females, males, and neomales. The expression was significantly ( $p < 0.05$ ) higher in neomales than in males and females, the latter of which had low levels of expression. In mice, loss of *wnt4* is sufficient to up-regulate *Fgf9* and results in partial testis development in XX gonads<sup>33</sup>. In humans, *wnt4* over-expression leads to up-regulated of *DAX1*, which results in an XY female phenotype<sup>48</sup>. Gonadal expression of *wnt4a* is higher in males than in females in rainbow trout<sup>17</sup>, marsupials<sup>45</sup>, and tongue sole, which is in contrast to the pattern during

gonadal development in mice and humans. Thus, *wnt4a* over-expression is associated with sex reversal.

To evaluate the mechanism of differential expression in gonads of males, females, and neomales, we measured the level of methylation in the first exon of *CS-wnt4a* in tongue sole. The level was highest in the gonads of females, moderate in males, and lowest in neomales. The level of methylation was negatively correlated with *CS-wnt4a* expression suggesting that methylation of the *CS-wnt4a* first exon was associated with the *CS-wnt4a* expression. In many species, DNA methylation inhibits expression of the target gene. For example, DNA methylation of *GATAD1* in humans decreases expression of *GATAD1*<sup>48</sup>. In European sea bass, DNA methylation of the *Cyp19a1* promoter decreases expression and induces masculinization<sup>49</sup>. In Japanese flounder, DNA methylation of *Dmrt1* and the *Cyp19a1* promoter results in sexual dimorphism<sup>50</sup>.

Table 1 | Likelihood ratio test (LRT) of branch-model and branch-site-models for *wnt4a* genes

Model	Np <sup>a</sup>	Ln likelihood	Parameter estimates	Model compare	Positive Selection site	2ΔlnL(p-value) <sup>b</sup>
<b>Branch model</b>						
1.One-ratio	71	-14470.28	$\omega = 0.036$			
2.Omega = 1	70	-17334.08	$\omega = 1$	2vs1		5727.6(p = 0)
3.Free-ratio	74	-14486.15	variable v by branch	3vs1		31.74(p = 5.93715E-07)
<b>Branch-site model</b>						
4:Null b	73	-14417.88				
5:b	74	-14415.45		3vs4	41,156**,179,181,347	4.86(p = 0.027)
6:Null-a	73	-14412.85				
7:a	74	-14406.24		5vs6	94,276	13.22(p = 0.000277)
8:Null-Mam <sup>c</sup>	73	-14419.26				
9:Mam	74	-14417.72		7vs8	Not allowed	3.08(p = 0.079)
10:Null-Tel <sup>d</sup>	73	-14419.26				
11:Tel	74	-14406.53		10vs9	3,4*,6,10,21*,33, 34,59,61,93, 96,232,281,296, 304,325,332,347	25.46(p = 4.51651E-07)

<sup>a</sup>Number of parameters.  
<sup>b</sup>Twice the difference of ln [likelihood] between the two models compared.  
<sup>c</sup>Mam = Ancestor branch of the mammals examined in present study.  
<sup>d</sup>Tel = Ancestor branch of the Teleosts examined in present study.  
The posterior probabilities  $p > 0.95$  and  $p > 0.99$  are indicated by \* and \*\*, respectively.

We constructed a phylogenetic tree based on the nucleotide sequences from 36 taxa to analyze the evolutionary context of *CS-wnt4a*. *CS-wnt4a* was genetically related to those of *Epinephelus coioides* (Fig. 3). The results of the phylogeny analysis were consistent with the highest amino acid sequence identity in the homolog comparison. Mammalian and teleost *wnt4a* genes formed one branch

and the teleost *wnt4b* gene formed another branch. We assumed that genome duplication in teleosts resulted in two *wnt4* genes and the *wnt4* subgroup likely originated very early during metazoan evolution<sup>17</sup>. Additionally, the high ratio of molecular evolution for many genes following the genome duplications in fish has resulted in functional shifts<sup>22</sup>. Therefore, *wnt4b* and *wnt4a* did not cluster together

Table 2 | Site model tests on *wnt4a* genes in mammalian and fish

Model	Np <sup>a</sup>	Ln likelihood	Parameter estimates	Model compare	Positive Selection site	2ΔlnL(p-value) <sup>b</sup>
<b>Mammalian</b>						
M0:one-ratio	15	-3063.91	$\omega = 0.056$			
M3:discrete	19	-3010.04	$\omega_0 = 0.000, p_0 = 0.213$ $\omega_1 = 0.000, p_1 = 0.586$ $\omega_2 = 0.339, p_2 = 0.201$	M3vsM0	Not found	107.74(p = 2.2075E-22)
M1a:nearly neutral	16	-3026.45	$\omega_0 = 0.020, p_0 = 0.909$ $\omega_1 = 1.000, p_1 = 0.090$			
M2a:positive selection	18	-3026.44	$\omega_0 = 0.020, p_0 = 0.909$ $\omega_1 = 1.000, p_1 = 0.070$ $\omega_2 = 1.000, p_2 = 0.020$	M2vsM1	Not allowed	0 (p = 1)
M7:β	16	-3011.21	$p = 0.091, q = 1.168$			
M8:β and ω	18	-3011.14	$p_0 = 0.994, p_1 = 0.006$ $\omega = 1.000, p = 0.094,$ $q = 1.306$	M8vsM7	Not allowed	0 (p = 1)
<b>Teleosts</b>						
M0:one-ratio	31	-5834.91	$\omega = 0.033$			
M3:discrete	35	-5728.44	$\omega_0 = 0.005, p_0 = 0.771$ $\omega_1 = 0.123, p_1 = 0.22$ $\omega_2 = 1.075, p_2 = 0.009$	M3vsM0	5,7,39**,94**	212.94(p = 6.193E-45)
M1a:nearly neutral	32	-5779.92	$\omega_0 = 0.026, p_0 = 0.978$ $\omega_1 = 1.000, p_1 = 0.022$			
M2a:positive selection	34	-5779.92	$\omega_0 = 0.026, p_0 = 0.978$ $\omega_1 = 1.000, p_1 = 0.022$ $\omega_2 = 40.005, p_2 = 0.00$	M2vsM1	Not allowed	0 (p = 1)
M7:β	32	-5739.53	$p = 0.18, q = 3.84$			
M8:β and ω	34	-5729.29	$p_0 = 0.993, p_1 = 0.007$ $\omega = 1.291, p = 0.214$ $q = 5.962$	M8vsM7	39,94	20.48(p = 3.5712E-5)

<sup>a</sup>Number of parameters.  
<sup>b</sup>Twice the difference of ln [likelihood] between the two models compared.  
The posterior probabilities  $p > 0.95$  and  $p > 0.99$  are indicated by \* and \*\*, respectively.

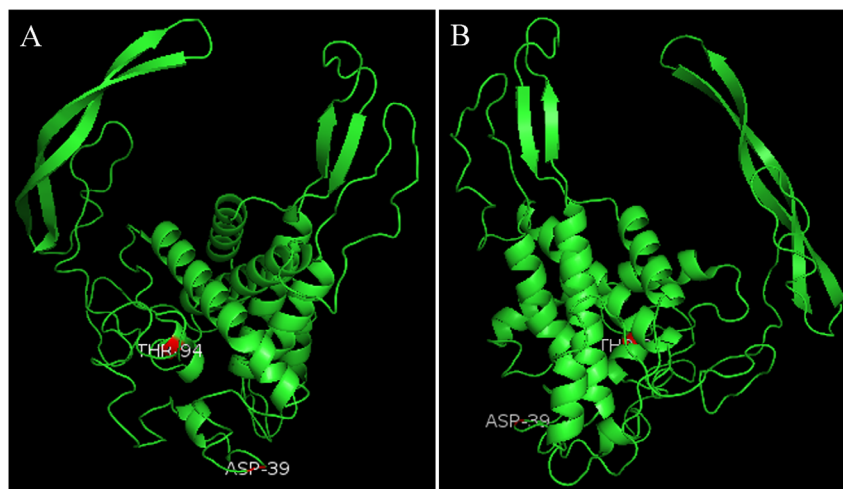


**Figure 4** | Three dimensional models of *CS-wnt4a* gene based on the tongue sole sequences. Images depicted represent two perspectives (the angles of view are  $0^\circ$  and  $180^\circ$ ). Shown is the positive selection sites (red). 94T positive selection sites located in the  $\alpha$ -helices; 39D located in the random coils.

on a single branch. Our phylogenetic tree was similar to that constructed for rainbow trout<sup>17</sup>.

To study the molecular evolution of the *wnt4* sequences, we constructed a series of models. The phylogenetic tree was also used to detect positive selection of *wnt4* sequences within the ancestral lineage of vertebrates, mammals, and teleosts. If the ratio of the non-synonymous nucleotide difference ( $d_N$ ) to the synonymous nucleotide difference ( $d_S$ ) between sequences was significantly greater than one, then positive selection was involved<sup>31</sup>. If the ratio of  $d_N/d_S(\omega)$  was significantly less than one, then purify selection is inferred. We compared the one-ratio model with the one-ratio model ( $\omega = 1$ ). The *wnt4* gene was strongly conserved and underwent purify selection ( $p < 0.01$ , Table 1). In general, most genes undergo purify selection whereas rare genes undergo position selection during evolution<sup>52</sup>. Subsequently, the free-ratio model was used to analyze the ratios among the different branches, revealing that each branch had independent  $d_N/d_S(\omega)$ . Additionally, a number of positive selection sites were detected in the different groups using the branch-site model. For example, we found 2 and 5 positively selected sites in *wnt4a* and *wnt4b*, respectively, in the ancestor vertebrate. Genome duplication occurred 320 million years ago in teleost fish, and the high rate of molecular evolution for many genes following genome duplication drove the functional shift<sup>24,43</sup>. We detected 18 positively selected sites in teleosts for the *wnt4a* gene. Rensch noted that positive selection is associated with a functional and environmental shift<sup>53</sup>. Thus, the positively selected sites in mammals and teleosts may be associated with occupation of different habitats, changes in oxygen consumption, or sex differentiation.

Additionally, we used a site model to detect positive selection. We detected 2 positively selected sites in teleosts, but none in mammals. Water represents a relative stable environment, thus selection pressure is thought to be weaker than in terrestrial environments and the rate of molecular evolution should be correspondingly lower<sup>53</sup>. However, our observations did not support this, likely because genome duplication resulted in two *wnt4* genes in teleosts (*wnt4a* and *wnt4b*), and the duplicate gene had a high rate of molecular evolution. Additionally, the *wnt4* gene is primarily expressed in the gonads, with expression being higher in the ovary than the testis in mammalian. In teleosts, *wnt4* gene RNA transcription is also higher in the ovary than in the testis in normal fish. However, the pattern is reversed in partial fish. As exemplified, Rainbow trout<sup>17</sup>, Zebrafish<sup>44</sup> and Tongue sole. Thus, the functional diversity in fish may be a result of *wnt4* gene evolution. As we known, positive selection plays a role in the diversification of protein function. Thus, we mapped the positively selected sites on the 3D structure to assess their biological

significance. We mapped one positively selected site on the  $\alpha$ -helices and the other positively selected sites on the random coils. The two positively selected sites were on the outside region of the 3D structure. This indicated that outside region may be necessary for protein function.

Teleosts occupy water of a wide range of salinities, which can have an effect on reproduction<sup>54–56</sup>. We speculated that as part of the adaptation to freshwater, the ancestral *wnt4* gene may have shifted its function by molecular evolution. Our observations of the positively selected *wnt4a* gene sites may be used to analyze genome duplication and the reproduction system in tongues sole.

## Methods

**Fish sampling and exposure to high temperature.** Healthy tongue sole were collected from the Haiyang 863 High-Tech Experiment Base (Haiyang, China). The tongue sole were acclimated to laboratory culture for at least one week. The fish were fed twice daily with commercial pellets. To determine the role of the *CS-wnt4a* gene in sex reversal, the tongue sole were treated at  $28^\circ\text{C}$  on day 23–30 after hatching until day 100, then reared to adulthood at a natural water temperature ( $22^\circ\text{C}$ )<sup>29</sup>. To determine the pattern of *CS-wnt4a* tissue expression, samples of one year old age were collected from the heart, liver, gill, skin, blood, kidney, intestine, brain, spleen, muscle, pituitary, ovary, and testis. Additionally, gonad samples were collected from healthy tongue sole throughout the rearing period (70D, 160D, 1Y, 2Y). The samples were immediately frozen in liquid nitrogen and then stored at  $-80^\circ\text{C}$  until RNA extraction. To visualize the location of RNA transcription in gonad cells, the gonad was fixed in 4% paraformaldehyde (PFA) and subject to *in situ* hybridization (ISH).

**Genetic sex and phenotypic sex.** To determine the genetic sex, genomic DNA was extracted from the fin samples of tongue sole using a standard phenol-chloroform method. The gonads were collected and fixed in Bouin's solution. The genetic sex and phenotype sex was identified followed Deng's description<sup>27</sup>.

**PCR amplification and cloning.** To obtain the full length cDNA sequence, one pair of primers (Wnt4a-5'GSP and Wnt4a-3'GSP) was designed according to the partial sequence which was obtained from our laboratory transcriptome data<sup>30</sup>. The PCR reaction mixture (50  $\mu\text{l}$ ) was prepared according to the manufacturer's instructions using a BD SMART<sup>TM</sup> RACE cDNA Amplification kit. The PCR reactions were performed under the following conditions: 5 cycles of  $94^\circ\text{C}$  for 30 s and  $72^\circ\text{C}$  for 3 min, 5 cycles of  $94^\circ\text{C}$  for 30 s,  $70^\circ\text{C}$  for 30 s, and  $72^\circ\text{C}$  for 3 min, then 27 cycles of  $94^\circ\text{C}$  for 30 s,  $68^\circ\text{C}$  for 30 s, and  $72^\circ\text{C}$  for 3 min. All of the amplification products were run on a 1% agarose gel using the D2000 marker (Takara, Dalian, China). The purified fragment was cloned into a PMD-18-T vector, inserted into *E. coli* TOP10, and then sequenced.

***CS-wnt4a* expression in tongue sole and localization in gonadal cells.** Samples from three individuals were mixed for RNA preparation. RNA was extracted from the various tissues, from the gonads collected at different stages, and from sex reversed gonads using Trizol (Qiagen, Dusseldorf, Germany) following the manufacturer's instruction. cDNA synthesis was performed using a QuantScript RT kit (Takara, Dalian, China) according to the manufacturer's protocol. The real-time RT-PCR primers were designed based on the *CS-wnt4a* gene sequence (Table S1). Real-time RT-PCR was performed on a 7500 real-time PCR system (Applied Biosystems),



California, USA) using 10 ml SYBR Premix Ex Taq (Takara, Dalian, China), 0.4 ml of Wnt4a-S1 and Wnt4a-A1, 1 ml cDNA, and 0.4 ml ROX reference dye following the manufacturer's protocol. PCR amplification was performed in triplicate wells and the conditions were as follows: 10 s at 95°C, followed 40 cycles at 95°C for 5 s and 60°C for 34 s. A dissociation curve analysis was performed to determine target specificity.  $\beta$ -Actin was used as the internal control. The standard curve was performed at three dilutions of the template (10, 100, and 1000 times). The concentration of cDNA in each sample was reflected by the crossing point (Ct) values, which were compared using the relative quantification method and 7500 system SDS software (Applied Biosystems, California, USA). The data were log-transformed. The transformed data were analyzed by one-way ANOVA followed by Duncan multiple comparison tests using SPSS 17.0 (IBM, New York, NY, USA). Significance was set at  $p < 0.05$ . To locate *CS-wnt4a* expression in the gonad cell, one pair of primers (Table S1) was designed for *in situ* hybridization (ISH) following the method described in Bhat<sup>57</sup>.

**Analysis of *CS-wnt4a* first exon methylation.** The majority of gonadal DNA methylation in half-smooth tongue sole occurred at the first exon of the gene<sup>25</sup>. The *CS-wnt4a* gene structure was determined using the complete cDNA sequence and the whole genome sequence<sup>30</sup>. A methylation primer was designed using online software <http://www.urogene.org/methprimer/index1.html>. To account for individual differences, we collected the gonads of eight females, eight males, and eight neomales for methylation analysis. The DNA was extracted and the concentration was quantified. Then, equimolar gonadal DNA from each individual was mixed in the same group. The mixed DNA was treated using a DNA methylation kit (Zymo, California, USA) and subject to PCR amplification following the manufacturer's protocol with the treated DNA as the reaction template. The purified fragment was cloned into a PMD-18-T vector and conveyed into *E. coli* TOP10. We then sequenced nine positive clones from each group.

**Sequences analysis, alignment, and phylogenetic analysis.** The *wnt4* cDNA sequences were obtained from the GenBank (<http://www.ncbi.nlm.nih.gov/>) and Ensemble (<http://www.ensembl.org/index.html>) databases, including 34 vertebrates and 2 invertebrates as the outgroup (Table S2). The signal was predicted by the online software <http://www.cbs.dtu.dk/services/SignalP/>, the protein conserved domain was identified by <http://www.ncbi.nlm.nih.gov/cdd/>, glycosylation sites were determined using <http://www.cbs.dtu.dk/services/NetOGlyc/>, and the methylation island was determined using <http://www.urogene.org/methprimer/>. The online software (<http://www.ebi.ac.uk/Tools/msa/muscle/>) was used to align the putative amino acid sequences. The jmodeltest 2 software was used to assess the optimal model for the nucleotide sequences under the Bayesian Information Criterion (BIC). The GTR+I+G model was selected as the best model to structure the phylogenetic tree using the Bayesian inference in MrBayes 3.1 with 25% tree burned under 5,000,000 generations. TreeView software was used to edit the phylogenetic tree.

**Evolutionary analysis.** The phylogenetic tree reconstructed using a Bayesian approach was analyzed to determine whether the environment had influenced the selective pressure on the ancestors of aquatic or terrestrial species. We performed a rigorous statistical analysis with *wnt4* gene sequences, including branch-specific dN/dS ratio tests, branch-site dN/dS ratio tests, and site-specific dN/dS ratio tests. All these analyses used the maximum likelihood (ML) method in the Codeml program of PAML version 4<sup>52</sup>. The maximum likelihood estimates the selective pressure via the nonsynonymous (dN) and synonymous (dS) nucleotide substitution rate ratio (dN/dS) with the  $dN/dS(\omega) = 1$  representing neutral evolution,  $\omega > 1$  representing positive selection, and  $\omega < 1$  representing purifying selection. First, the one-ratio model was used to assess the selective pressure among all *wnt4* genes. Then, the free model was used to determine whether every branch allows the varied  $\omega$  ratio via the likelihood ratio test by comparing with the one ratio model. Additionally, the branch-site model was used to detect the interested foreground lineage. A total of six site models were used to test for positive selection in individual codons of *wnt4* sequences. A two-fold difference in the log-likelihood values ( $2\Delta\ln L$ ) between the two nested models was calculated using a chi-square test with the degrees of freedom equal to the difference in the number of parameters between the nested models. The Bayes empirical Bayes (BEB) was used to assess the Bayesian posterior probability (BPP) of the site model under positive selection. To present the result of our study more visualized, three dimensional models of *CS-wnt4a* which can map the positively selected sites was constructed by the iterative threading assembly refinement (I-TASSER) server<sup>58</sup>. The PYMOL software v1.5 was used to analyze the structure.

- Bernard, P. & Harley, V. R. Wnt4 action in gonadal development and sex determination. *Int J Biochem Cell Biol* **39**, 31–43 (2007).
- Vainio, S., Heikkilä, M., Kispert, A., Chin, N. & McMahon, A. P. Female development in mammals is regulated by Wnt-4 signalling. *Nature* **397**, 405–409 (1999).
- Jeays-Ward, *et al.* Endothelial and steroidogenic cell migration are regulated by WNT4 in the developing mammalian gonad. *Development* **130**, 3663–3670 (2003).
- Biason-Lauber, A., Konrad, D., Navratil, F. & Schoenle, E. J. A WNT4 mutation associated with Mullerian-duct regression and virilization in a 46 XX woman. *N. Engl. J. Med* **351**, 792–798 (2004).
- Elejalde, B. R. *et al.* Tandem dup (1p) within the short arm of chromosome 1 in a child with ambiguous genitalia and multiple congenital anomalies. *Am J Med Genet* **17**, 723–730 (1984).
- Mohammed, F. M. *et al.* Direct duplication of chromosome 1, dir dup(1)(p21.2–p32) in a Bedouin boy with multiple congenital anomalies. *Am. J. Med. Genet* **32**, 353–355 (1989).
- Deshpande, S. N., Vijayakumar, G. & Rao, A. J. Oestrogenic regulation and differential expression of WNT4 in the bonnet monkey and rodent epididymis. *Reprod Biomed Online* **18**, 555–561 (2009).
- Pask, A. J., Calatayud, N. E., Shaw, G., Wood, W. M. & Renfree, M. B. Oestrogen blocks the nuclear entry of SOX9 in the developing gonad of a marsupial mammal. *BMC Biol* **8**, 113 (2010).
- Pailhoux, E. *et al.* Ontogenesis of female-to-male sex-reversal in XX polled goats. *Dev Dyn* **224**, 39–50 (2002).
- Jeays-Ward, K., Dandonneau, M. & Swain, A. Wnt4 is required for proper male as well as female sexual development. *Dev Biol* **276**, 431–440 (2004).
- Jordan, B. K., Shen, J. H., Olosa, R., Ingraham, H. A. & Vilain, E. Wnt4 over expression disrupts normal testicular vasculature and inhibits testosterone synthesis by repressing steroidogenic factor 1/beta-catenin synergy. *Proc Natl Acad Sci U S A* **100**, 10866–10871 (2003).
- Jameson, S. A., Lin, Y. T. & Capel, B. Testis development requires the repression of Wnt4 by Fgf signaling. *Dev Biol* **370**, 24–32 (2012).
- Janssen, R. & Posnien, N. Identification and embryonic expression of Wnt2, Wnt4, Wnt5 and Wnt9 in the millipede *Glomeris marginata* (Myriapoda: Diplopoda). *Gene Expr Patterns* **14**, 55–61 (2014).
- Oshima, Y., Hayashi, T., Tokunaga, S. & Nakamura, M. Wnt4 expression in the differentiating gonad of the frog *Rana rugosa*. *Zoolog Sci* **22**, 689–693 (2005).
- Tripathi, V. & Raman, R. Identification of Wnt4 as the ovary pathway gene and temporal disparity of its expression vis-a-vis testis genes in the garden lizard, *Calotes versicolor*. *Gene* **449**, 77–84 (2010).
- Smith, C. A. *et al.* Cloning and expression of R-Spondin1 in different vertebrates suggests a conserved role in ovarian development. *BMC Dev Biol* **8**, 72 (2008).
- Nicol, B., Guerin, A., Fostier, A. & Guiguen, Y. Ovary-predominant wnt4 expression during gonadal differentiation is not conserved in the rainbow trout (*Oncorhynchus mykiss*). *Mol Reprod Dev* **79**, 51–63 (2012).
- Wu, G. C. & Chang, C. F. Wnt4 is associated with the development of ovarian tissue in the protandrous black Porgy, *Acanthopagrus schlegelii*. *Biol Reprod* **81**, 1073–1082 (2009).
- Lynch, M. & Conery, J. S. The evolutionary fate and consequences of duplicate genes. *Science* **290**, 1151–1155 (2000).
- Hughes, A. L. The evolution of functionally novel proteins after gene duplication. *Proc Biol Sci* **256**, 119–124 (1994).
- Assis, R. & Bachtrog, D. Neofunctionalization of young duplicate genes in *Drosophila*. *Proc Natl Acad Sci U S A* **110**, 17409–17414 (2013).
- Steinke, D., Salzburger, W., Braasch, I. & Meyer, A. Many genes in fish have species-specific asymmetric rates of molecular evolution. *BMC Genomics* **7**, 20 (2006).
- Chen, S. L. *et al.* Isolation of female-specific AFLP markers and molecular identification of genotypic sex in half-smooth tongue sole (*Cynoglossus semilaevis*). *Mar Biotechnol* **9**, 273–280 (2007).
- Hu, Q. M. *et al.* Differences in sex reversion and growth between normal and neomale stock in half-smooth tongue sole. *Cynoglossus semilaevis. Aquacult Int* **22**, 1437–1449 (2014).
- Shao, C. W. *et al.* Epigenetic modification and inheritance in sexual reversal of fish. *Genome Res* **24**, 604–615 (2014).
- Dong, X. L., Chen, S. L., Ji, X. S. & Shao, C. W. Molecular cloning, characterization and expression analysis of Sox9a and Foxl2 genes in half-smooth tongue sole (*Cynoglossus semilaevis*). *Acta Oceanol. Sin* **30**, 68–77 (2011).
- Deng, S. P., Chen, S. L., Xu, J. Y. & Liu, B. W. Molecular cloning, characterization and expression analysis of gonadal P450 aromatase in the half-smooth tongue-sole, *Cynoglossus semilaevis*. *Aquaculture* **287**, 211–218 (2009).
- Deng, S. P., Chen, S. L. & Liu, B. W. Molecular cloning and expression analysis of FTZ-F1 in the half-smooth tongue sole. *Cynoglossus semilaevis. Zoological Research* **29**, 592–598 (2008).
- Hu, Q. M. & Chen, S. L. Cloning, genomic structure and expression analysis of *ubc9* in the course of development in the half-smooth tongue sole (*Cynoglossus semilaevis*). *Comp Biochem Physiol B Biochem Mol Biol* **165**, 181–188 (2013).
- Chen, S. L. *et al.* Whole-genome sequence of a flatfish provides insights into ZW sex chromosome evolution and adaptation to a benthic lifestyle. *Nat Genet* **46**, 253–260 (2014).
- Inohaya, K., Takano, Y. & Kudo, A. Production of Wnt4b by floor plate cells is essential for the segmental patterning of the vertebral column in medaka. *Development* **137**, 1807–1813 (2010).
- Kim, Y. *et al.* Fgf9 and wnt4 act as antagonistic signals to regulate mammalian sex determination. *PLoS Biol* **4**, e187 (2006).
- García-Castro, B. *et al.* Restoration of WNT4 inhibits cell growth in leukemia-derived cell lines. *BMC Cancer* **13**, 557 (2013).
- DiRocco, D. P., Kobayashi, A., Taketo, M. M., McMahon, A. P. & Humphreys, B. D. Wnt4/ $\beta$ -catenin signaling in medullary kidney myofibroblasts. *J Am Soc Nephrol* **24**, 1399–412 (2013).





35. Prunskaitė-Hyyryläinen, R. *et al.* Wnt4, a pleiotropic signal for controlling cell polarity, basement membrane integrity, and antimüllerian hormone expression during oocyte maturation in the female follicle. *FASEB J* **28**, 1568–81 (2013).
36. B.Parekh, R. Effects of glycosylation on protein function. *Curr Opin Struct Biol* **1**, 750–754 (1991).
37. Moremen, K. W., Tiemeyer, M. & Nairn, A. V. Vertebrate protein glycosylation: diversity, synthesis and function. *Nat Rev Mol Cell Biol* **13**, 448–462 (2012).
38. Graba, Y. *et al.* DWnt4, a novel Drosophila Wnt gene acts downstream of homeotic complex genes in the visceral mesoderm. *Development* **121**, 209–218 (1995).
39. Ferkowicz, M. J., Stander, M. C. & Raff, R. A Phylogenetic relationships and developmental expression of three sea urchin Wnt genes. *Mol Biol Evol* **15**, 809–819 (1998).
40. Shan, J., Jokela, T., Peltoketo, H. & Vainio, S. Generation of an allele to inactivate Wnt4 gene function conditionally in the mouse. *Genesis* **47**, 782–788 (2009).
41. Ungar, A. R., Kelly, G. M. & Moon, R. T. Wnt4 affects morphogenesis when misexpressed in the zebrafish embryo. *Mech Dev* **52**, 153–164 (1995).
42. Meyer, A. & Van de Peer, Y. From 2R to 3R: Evidence for a fish-specific genome duplication (FSGD). *Bioessays* **27**, 937–945 (2005).
43. Delsuc, F., Brinkmann, H. & Philippe, H. Phylogenomics and the reconstruction of the tree of life. *Nat Rev Genet* **6**, 361–375 (2005).
44. Matsui, T. *et al.* Noncanonical Wnt signaling regulates midline convergence of organ primordia during zebrafish development. *Genes Dev* **19**, 164–175 (2005).
45. Yu, H. S., Pask, A. J., Shaw, G. & Renfree, M. B. Differential expression of WNT4 in testicular and ovarian development in a marsupial. *BMC Dev Biol* **6**, 44 (2006).
46. Jordan, B. K., Shen, J. H., Olaso, R., Ingraham, H. A. & Vilain, E. Wnt4 over-expression disrupts normal testicular vasculature and inhibits testosterone synthesis by repressing steroidogenic factor 1/beta-catenin synergy. *Proc Natl Acad Sci USA* **100**, 10866–10871 (2003).
47. Jordan, B. K. *et al.* Up-regulation of WNT-4 signaling and dosage-sensitive sex reversal in humans. *Am J Hum Genet* **68**, 1102–1109 (2001).
48. Ma, X., Li, J., Brost, B., Cheng, W. & Jiang, S. W. Decreased expression and DNA methylation levels of GATAD1 in preclimptic placentas. *Cell Signal* **26**, 959–967 (2014).
49. Navarro-Martín, L. *et al.* DNA methylation of the gonadal aromatase (cyp19a) promoter is involved in temperature-dependent sex ratio shifts in the European sea bass. *PLoS Genet* **7**, e1002447 (2011).
50. Wen, A. Y. *et al.* CpG methylation of dmrt1 and cyp19a promoters in relation to their sexual dimorphic expression in the Japanese flounder *Paralichthys olivaceus*. *J Fish Biol* **84**, 193–205 (2014).
51. Hughes, A. L. & Nei, M. Pattern of nucleotide substitution at major histocompatibility complex class I loci reveals overdominant selection. *Nature* **335**, 167–170 (1988).
52. Yang, Z. H. PAML 4: phylogenetic analysis by maximum likelihood. *Mol Biol Evol* **24**, 1586–1591 (2007).
53. Rensch, B. Evolution Above The Species Level. New York:Columbia Univ.Press. 124P(1960).
54. Yen, P. T. & N. Bart, A. Salinity effects on reproduction of giant freshwater prawn *Macrobrachium rosenbergii* (de Man). *Aquaculture* **280**, 124–128 (2008).
55. L. Ohsa C, L. Rhyneb, A. W. & Grabe, S. Effects of salinity on reproduction and survival of the calanoid copepod *Pseudodiaptomus pelagicus*. *Aquaculture* **307**, 219–224 (2010).
56. Nissling, A., Johansson, U. & Jacobsson, M. Effects of salinity and temperature conditions on the reproductive success of turbot (*Scophthalmus maximus*) in the Baltic Sea. *Fish Res* **80**, 230–238 (2006).
57. Bhat, N. & Hong, Y. H. Cloning and expression of boule and dazl in the Nile tilapia (*Oreochromis niloticus*). *Gene* **540**, 140–145 (2014).
58. Roy, A., Kucukural, A. & Zhang, Y. I-TASSER: a unified platform for automated protein structure and function prediction. *Nat. Protoc.* **5**, 725–738 (2010).

## Acknowledgments

This work was supported by State 863 High-Technology R&D Project of China (2012AA092203;2012AA10A403-2), National Nature Science Foundation (31130057), and Taishan Scholar Project Fund of Shandong of China.

## Author contributions

Q.M.H. and S.L.C. conceived and designed the experiments. Q.M.H., Y.Z. and Y.L. performed the experiments. Q.M.H. and N.W. analyzed the data. Q.M.H. and S.L.C. wrote the paper. All authors reviewed the manuscript.

## Additional information

Supplementary information accompanies this paper at <http://www.nature.com/scientificreports>

Competing financial interests: The authors declare no competing financial interests.

How to cite this article: Hu, Q., Zhu, Y., Liu, Y., Wang, N. & Chen, S. Cloning and characterization of *wnt4a* gene and evidence for positive selection in half-smooth tongue sole (*Cynoglossus semilaevis*). *Sci. Rep.* **4**, 7167; DOI:10.1038/srep07167 (2014).



This work is licensed under a Creative Commons Attribution-NonCommercial-ShareAlike 4.0 International License. The images or other third party material in this article are included in the article's Creative Commons license, unless indicated otherwise in the credit line; if the material is not included under the Creative Commons license, users will need to obtain permission from the license holder in order to reproduce the material. To view a copy of this license, visit <http://creativecommons.org/licenses/by-nc-sa/4.0/>